BIOLOGY OF REPRODUCTION **84,** 255–265 (2011)
Published online before print 22 September 2010.
DOI 10.1095/biolreprod.110.086942

Altered Spatiotemporal Expression of Collagen Types I, III, IV, and VI in *Lpar3*-Deficient Peri-Implantation Mouse Uterus[1]

Honglu Diao,[3] John D. Aplin,[5] Shuo Xiao,[3,4] Jerold Chun,[6] Zuguo Li,[3] Shiyou Chen,[3] and Xiaoqin Ye[2,3,4]

Department of Physiology and Pharmacology,[3] College of Veterinary Medicine, and Interdisciplinary Toxicology Program,[4] University of Georgia, Athens, Georgia
Maternal and Fetal Health Research Group,[5] Manchester Academic Health Sciences Centre, St. Mary's Hospital, University of Manchester, Manchester, United Kingdom
Department of Molecular Biology,[6] Dorris Neuroscience Center, The Scripps Research Institute, La Jolla, California

ABSTRACT

***Lpar3* is upregulated in the preimplantation uterus, and deletion of *Lpar3* leads to delayed uterine receptivity in mice. Microarray analysis revealed that there was higher expression of *Col3a1* and *Col6a3* in the Preimplantation Day 3.5 *Lpar3*$^{-/-}$ uterus compared to Day 3.5 wild-type (WT) uterus. Since extracellular matrix (ECM) remodeling is indispensable during embryo implantation, and dynamic spatiotemporal alteration of specific collagen types is part of this process, this study aimed to characterize the expression of four main uterine collagen types: fibril-forming collagen (COL) I and COL III, basement membrane COL IV, and microfibrillar COL VI in the peri-implantation WT and *Lpar3*$^{-/-}$ uterus. An observed delay of COL III and COL VI clearance in the *Lpar3*$^{-/-}$ uterus may be associated with higher preimplantation expression of *Col3a1* and *Col6a3*. There was also delayed clearance of COL I and delayed deposition of COL IV in the decidual zone in the *Lpar3*$^{-/-}$ uterus. These changes were different from the effects of 17beta-estradiol and progesterone on uterine collagen expression in ovariectomized WT uterus, indicating that the altered collagen expression in *Lpar3*$^{-/-}$ uterus is unlikely to be a result of alterations in ovarian hormones. Decreased expression of several genes encoding matrix-degrading metallo- and serine proteinases was observed in the *Lpar3*$^{-/-}$ uterus. These results demonstrate that pathways downstream of LPA3 are involved in the dynamic remodeling of ECM in the peri-implantation uterus.**

collagen types I, III, IV, and VI, decidua, endometrium, female reproductive tract, implantation, lysophosphatidic acid receptor 3, pregnancy, uterus

INTRODUCTION

Collagens, the main protein components of extracellular matrix (ECM), provide tissues with their strength and shape. In addition to their structural functions, collagens act as ligands for cell membrane receptors (e.g., integrins and annexin A5) through which they mediate cellular functions, such as growth, survival, differentiation, adhesion, and migration [1, 2]. There are at least 28 different collagen subtypes classified into eight subfamilies: fibril-forming collagen (e.g., collagen [COL] I); basement membrane collagen (e.g., COL IV); beaded filament-forming collagen (e.g., COL VI); anchoring fibril-forming collagen (e.g., COL VII); fibril-associated collagens with interruptions in triple helix (COL IX); hexagonal network-forming collagens (e.g., COL X); transmembrane collagens (e.g., COL XIII); and multiplexins (e.g., COL XVIII) [2].

Uterine collagen content alters during pregnancy and postpartum involution [3]. In the embryo implantation phase of early pregnancy, progressive differentiation of fibroblast-like stromal cells into hypertrophic polygonal decidual cells correlates with profound alterations in collagen gene expression [4–7]. It has been demonstrated that different collagen types have distinct spatiotemporal expression patterns during implantation. The major fibril-forming COL I, III, and V are all reduced in implantation sites compared to non-implantation sites in the rat uterus [4], mainly because they progressively disappear from the primary and secondary decidual zones from Day 5.5 to Day 7.5 (Day 0 as mating night) [5–7]. Their expression patterns in the outer nondecidualized stroma and myometrial tissues do not seem to change during this period [5, 6]. COL IV is also a main endometrial ECM component [8], disappearing in the luminal epithelial basement membrane at implantation site [9], but accumulating in the decidual zone [10]. COL VI is lost from rat stromal cells undergoing decidualization [11]. It has been suggested that abnormally increased deposition of collagen might impair uterine function, possibly by interfering with vascularization [12] or retarding remodeling events at implantation.

Uterine ECM remodeling is regulated by hormones and local factors; 17β-estradiol (E2) can inhibit the loss of collagen from the involuting rat uterus in vivo [13], which reflects the inhibitory role of E2 on collagenase activity [14]. Progesterone (P4) was also shown to have an inhibitory effect on collagenase activity, preventing collagen degradation in postpartum rat uterine explants [15]. RU486, an antagonist and partial agonist of progesterone receptor (PR), can reduce COL IV expression in the Rhesus monkey decidua and villus during the first trimester of pregnancy [16]. It has been suggested that the spatiotemporal variation of PR and estrogen receptor in the uterus and cervix controls P4 and E2 action at parturition [17, 18], perhaps by regulating matrix metalloproteinases (MMPs), their inhibitors, and matrix-degrading serine proteinases [1, 19–23].

Lysophosphatidic acid (LPA) is a small lipid signaling molecule. Several reports have revealed potential roles of LPA on collagen regulation. LPA can induce collagen matrix contraction [24], and has a potential role in promoting wound healing [25], in which ECM deposition is a key event. LPA can

[1]Supported by startup funding from University of Georgia to X.Y. and by National Institutes of Health grant HD050685 to J.C.
[2]Correspondence: Xiaoqin Ye, Department of Physiology and Pharmacology, College of Veterinary Medicine & Interdisciplinary Toxicology Program, University of Georgia, Athens, GA 30602.
FAX: 706 542 3015; e-mail: ye@uga.edu

Received: 28 June 2010.
First decision: 2 August 2010.
Accepted: 16 September 2010.

eISSN: 1529-7268 http://www.biolreprod.org
ISSN: 0006-3363

also counteract transforming growth factor-β-induced COL I mRNA stabilization in dermal fibroblasts, therefore potentially preventing excessive scarring [26]. On the other hand, LPA may increase the invasiveness of ovarian cancer by upregulating MMP activity [27].

LPA functions through its G protein-coupled receptors [28, 29]. It was previously demonstrated that deletion of *Lpar3* leads to implantation defects [30, 31]. Since uterine *Lpar3* expression peaks at Preimplantation Day 3.5, this day was chosen to screen differentially expressed genes in *Lpar3*$^{-/-}$ uterus. Microarray results indicated higher *Col3a1* and *Col6a3* mRNA levels in the Preimplantation Day 3.5 *Lpar3*$^{-/-}$ uterus. This led us to investigate the expression of four representative collagen types in the uterus: fibril-forming COL I and COL III, basement membrane COL IV, and microfibril-forming COL VI, in the peri-implantation wild-type (WT) and *Lpar3*$^{-/-}$ uterus.

MATERIALS AND METHODS

Reagents

The following reagents were obtained as indicated in parentheses: TRIZOL and Superscript III (Invitrogen, Carlsbad, CA); dNTPs (Biomega, San Diego, CA); Taq DNA polymerase (Lucigen, Middleton, WI); E2 and progesterone (P4) (Sigma-Addrich, St. Louis, MO); superfrost plus slides (Fisher Scientific, Pittsburgh, PA); power SYBR green PCR master and 384-well plates (Applied Biosystems, Carlsbad, CA); goat anti-COL I and anti-COL III antibodies (SouthernBiotech, Birmingham, AL); rabbit anti-COL IV and anti-COL VI antibodies (Abcam, Cambridge, MA); goat IgG and rabbit IgG (Santa Cruz Biotechnology, Santa Cruz, CA); rat-anti-platelet/endothelial cell adhesion molecule (PECAM) and goat anti-rat Cy3 (gifts from Dr. Lianchun Wang at University of Georgia); Alexa Fluor 488 goat anti-rabbit IgG and Alexa Fluor 488 rabbit-anti goat IgG (Invitrogen, Carlsbad, CA); DAPI (4′,6′-diamidino-2-phenylindole) (MP Biomedicals, Solon, OH); Vectashield (Vector Labs, Burlingame, CA).

Animals

WT and *Lpar3*$^{-/-}$ mice (129/SvJ and C57BL/6 mixed background) were generated from a colony at the University of Georgia, which was originally derived from our colony at the Scripps Research Institute [30]. They were genotyped as previously described [30]. The mice were housed in polypropylene cages with free access to regular food and water from water sip tubes in a reverse-osmosis system. The animal facility is on a 12L:12D (0600–1800 h) at 23 ± 1°C with 30%–50% relative humidity. All methods used in this study were approved by the Animal Subjects Programs of the University of Georgia and conformed to National Institutes of Health guidelines and public law.

Mating and Uterine Tissue Collection

Young virgin (2–4 mo old) WT and *Lpar3*$^{-/-}$ females were mated naturally with WT stud males and checked for a vaginal plug the next morning. The day on which a vaginal plug was identified was designated as Day 0.5 (mating night as Day 0). Uterine tissues were collected between 1100 and 1200 h on Days 0.5, 3.5, 4.5, and 5.5, as well as between 2300 and 2400 h on Day 5.0. Day 0.5 females were euthanized with CO_2 inhalation, and both uterine horns were quickly removed and snap frozen on dry ice. Oviducts from these mice were dissected for the presence of eggs to determine the pregnancy status. Parts of uterine horns from euthanized Day 3.5 WT and *Lpar3*$^{-/-}$ females were quickly removed and frozen on dry ice for immunofluorescence, and the remainder flushed with 1× PBS (to determine the status of pregnancy and to remove embryos before examination of uterine gene expression) and frozen on dry ice for microarray analysis and real-time PCR. The uterine horns from Day 4.5, 5.0, and 5.5 WT and *Lpar3*$^{-/-}$ females were flash frozen. Sections with embryo(s) were used for immunofluorescence. Uterine horns from different Day 4.5 WT and *Lpar3*$^{-/-}$ females were fixed in 10% formalin for 24 h at room temperature for histology. At least three pregnant mice were included in each group.

Ovariectomy and Hormonal Treatment

WT virgin females (6 wk old) were ovariectomized and allowed to recover for 2 wk to eliminate ovarian steroids from the circulation. The ovariectomized mice received s.c. injection of vehicle (sesame oil), E2 (100 ng), or P4 (2 mg) in 0.1 ml vehicle daily. The mice were dissected 6, 24, or 72 h after the first injection. Uterine tissues were quickly removed and frozen on dry ice for immunofluorescence.

Total RNA Isolation, Microarray Analysis, and Real-Time PCR

To isolate total RNA for microarray analysis and real-time PCR, Day 3.5 WT and *Lpar3*$^{-/-}$ uterine horns were powdered in liquid nitrogen with a mortar and pestle. The powdered sample was quickly transferred to Trizol for total RNA isolation. Microarray analysis using mouse Illumina Chip was performed at the Genomics and Proteomics Core Facility, Medical College of Georgia, as previously described [32], with three replicates in each group. For real-time PCR, cDNA was transcribed from 1 μg of total RNA using Superscript III reverse transcriptase with random primers. Real-time PCR reactions were performed in 384-well plates using Sybr-Green I intercalating dye on ABI 7900 (Applied Biosystems). The primers (Integrated DNA Technologies) were: glyceraldehyde 3-phosphate dehydrogenase (*Gapdh*) e3F1, 5′-GCCGAGAATGGGAAGCTTGTCAT-3′; *Gapdh* e4R1, 5′-GTGGTTCACACCCATCACAAACAT-3′; *Col3a1* e2F1, 5′-GATGTCTGGAAGCCAGAAC-3′; *Col3a1* e4R1, 5′-TCACCATTTCTCCCAGGAA-3′; *Col6a3* e8F1, 5′-GTCCGAACTGAGTGAGACAG-3′; *Col6a3* e9R1, 5′-CTGGTACAACTTCAGCGTGT-3′. *Cma1* e3F1, 5′-GTCCACGACATCATGCTACT-3′; *Cma1* e4R1, 5′-GCTCCTGGAGTCTCATCTTT-3′; *Mcp4* e2F1, 5′-AGAGAGGGTTCACAGCTACC-3′; *Mcp4* e4R1, 5′-GGCCTCTTTATCCATGATTC-3′; *Mcp6* e3F2, 5′-CAGCTTCGTGAGCAGTATCT-3′; *Mcp6* e4R2, 5′-GTATTTCCAGCACACAGCAT-3′; *Mmp3* e4F1, 5′-AATGGAGATGCTCACTTTGA-3′; *Mmp3* e7R1, 5′-AGGAGTCCTGAGAGATTTGC-3′; *Mmp7* e2F1, 5′-TCACTAATGCCAAACAGTCC-3′; *Mmp7* e5R1, 5′-TGACTCAGACCCAGAGAGTG-3′; hypoxanthine phosphoribosyltransferase 1 (*Hprt1*) e3F1, 5′-GCTGACCTGCTGGATTACAT-3′; and *Hprt1* e4/5R1, 5′-CAATCAAGACATTCTTTCCAGT-3′.

Histology

Fixed Day 4.5 WT and *Lpar3*$^{-/-}$ uterine horns were embedded in paraffin and sectioned (4 μm) longitudinally in order to increase the chance of obtaining sections with embryo(s), especially from *Lpar3*$^{-/-}$ uteri that didn't show implantation sites at Day 4.5 [30]. Sections were deparaffinized, rehydrated, and stained with hematoxylin and eosin, as previously described [33].

Immunofluorescence

Frozen uterine horns from Days 0.5, 3.5, and 5.5 WT and *Lpar3*$^{-/-}$ females were cross-sectioned (10 μm) with the Day 5.5 sections crossing implantation sites. Frozen uterine horns from Days 4.5 and 5.0 WT and *Lpar3*$^{-/-}$ females were sectioned (10 μm) longitudinally in order to increase the chance of obtaining sections with embryo(s). Only the sections with embryo(s) from Day 4.5, 5.0, and 5.5 were used in the study. The frozen uterine sections on superfrost plus slides were fixed in freshly prepared 4% paraformaldehyde in 0.02 M PBS at room temperature (RT) for 20 min. The slides were washed in PBS three times for 5 min each. Sections for COL I and COL III (but not COL IV or COL VI) immunofluorescence underwent antigen retrieval before they were subsequently incubated in 0.2% Triton-X100/PBS for 20 min, and washed three times in PBS for 5 min each. Nonspecific staining was blocked with 10% rabbit (for COL I and COL III) or goat (for COL IV and COL VI) serum in PBS for 60 min at 37°C. Sections were incubated with primary goat anti-collagen antibody (1:25 for COL I and COL III) or rabbit anti-collagen antibody (1:400 for COL IV, and 1:500 for COL VI), and, in a few cases, with rat anti-PECAM (1:200) also, in blocking reagent at 4°C overnight. They were washed three times in PBS for 10 min each, incubated with Alexa Fluor 488 rabbit anti-goat IgG, Alexa Fluor 488 goat anti-rabbit IgG, or goat anti-rat Cy3 (1:200) in 1% BSA/PBS for 60 min at RT, then washed in PBS twice for 5 min each. They were then incubated with DAPI in PBS for 15 min at 37°C, and washed in PBS three times for 5 min each. The sections were mounted in Vectashield. Sections for negative control were processed exactly the same, except that the primary antibodies were replaced with goat IgG (for COL I and COL III) or rabbit IgG (for COL IV and COL VI).

Statistical Analyses

Statistical analyses were performed using two-tail, unequal variance Student *t*-test. The significant level was set at $P < 0.05$.

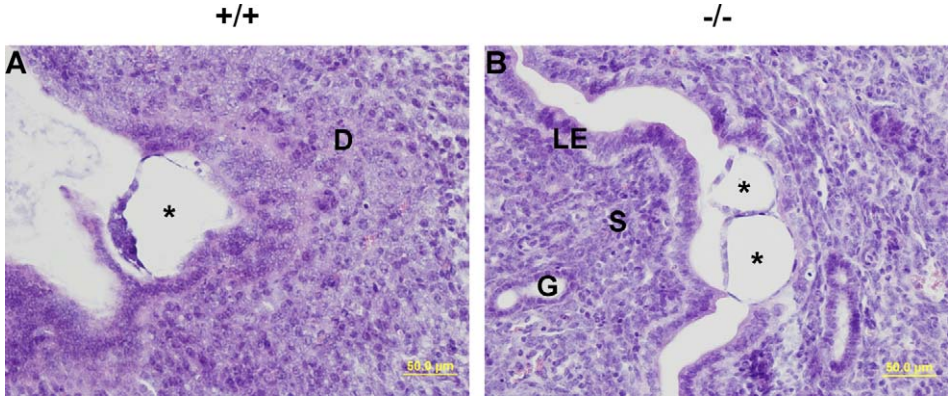

FIG. 1. Histology of Day 4.5 uterus with embryos. **A**) WT (+/+) uterus. **B**) *Lpar3*$^{-/-}$ uterus (−/−). The LE next to the embryos in **B** still maintains a single layer structure, and the stroma beneath lacks a primary decidual zone; the presence of two adjacent embryos in **B** is an early indication of embryo crowding in *Lpar3*$^{-/-}$ uterus [30]. H&E stain, 4-μm longitudinal section of formalin-fixed uterus. *Embryo; D, decidual zone. Bar = 50 μm; n = 3.

RESULTS

Histology of Day 4.5 WT and Lpar3$^{-/-}$ *Uterus*

It was demonstrated previously that deletion of *Lpar3* in mice leads to delayed implantation [30]. Histological examination on Day 4.5 revealed that the WT luminal epithelium (LE) had lost the single-layer epithelial morphology at the implantation site, and the subepithelial stroma had undergone morphological changes to form a primary decidual zone (Fig. 1A). In contrast, the LE opposed to blastocysts in the *Lpar3*$^{-/-}$ uterus maintained a single-layer epithelium, although cells were flattened and less dense than the adjacent LE; in addition, no decidual changes were apparent in the subepithelial stroma of *Lpar3*$^{-/-}$ uterus (Fig. 1B). These morphological differences suggest that the LE morphological changes and ECM remodeling associated with early implantation may be retarded in the *Lpar3*$^{-/-}$ uterus, consistent with delayed uterine receptivity [30].

Differential Expression of Col3a1 *and* Col6a3 *mRNA in Day 3.5* Lpar3$^{-/-}$ *Uterus*

Lpar3 expression in the WT uterus peaks at Preimplantation Day 3.5 [30]. Microarray analysis was performed to determine differentially expressed genes in the Day 3.5 *Lpar3*$^{-/-}$ whole uterus. *Col3a1* and *Col6a3* mRNA appeared more abundant in *Lpar3*$^{-/-}$ than in WT uterus, and these differential expressions were confirmed by real-time PCR (Fig. 2). It has been demonstrated that there is loss of COL III and COL VI (both protein and mRNA) in the decidual zone upon implantation in rodents [6, 11, 34]. No other collagen genes showed significantly differential expression in the microarray. We therefore examined the regulation of COL III and COL VI protein by ovarian hormones in WT uterus and their expression in the Peri-implantation Day 0.5, 3.5, 4.5, 5.0, and 5.5 WT and *Lpar3*$^{-/-}$ uterus. We compared two other main collagen types in the uterus—COL I and COL IV.

Regulation of Uterine COL III, I, VI, and IV by E2 and P4

COL III, I, VI, and IV are differentially regulated by ovarian hormones E2 and P4 in the ovariectomized WT uterus. Supplemental Figure S1 (all supplemental data are available at www.biolreprod.org) shows that COL III was detected in stroma and myometrium, but not in the epithelial compartment. In the oil-treated control uterus, COL III fibers appeared as fine granular staining with some connections with adjacent foci (Supplemental Fig. S1, A and B). No obvious changes were observed after 6 h of E2 or P4 treatment (data not shown). However, after 24 hours of E2 (but not P4) treatment, the COL III fibrils became thicker and longer, and appeared web-like (Supplemental Fig. S1, C and E), which persisted after 72 h of E2 treatment, and also showed up after 72 hours of P4 treatment (Supplemental Fig. S1, D and F). COL I staining and regulation by E2 and P4 were similar to COL III (Supplemental Fig. S1), except that the effects were delayed (images not shown; see summary in Table 1). Supplemental Figure S2 shows that COL VI was detected in the intercellular spaces of stroma and myometrium, and appeared as irregular punctuate deposits in the oil-treated uterus (Supplemental Fig. S2, A and B). After E2 or P4 treatment for 6 h (data not shown), a fibrillar

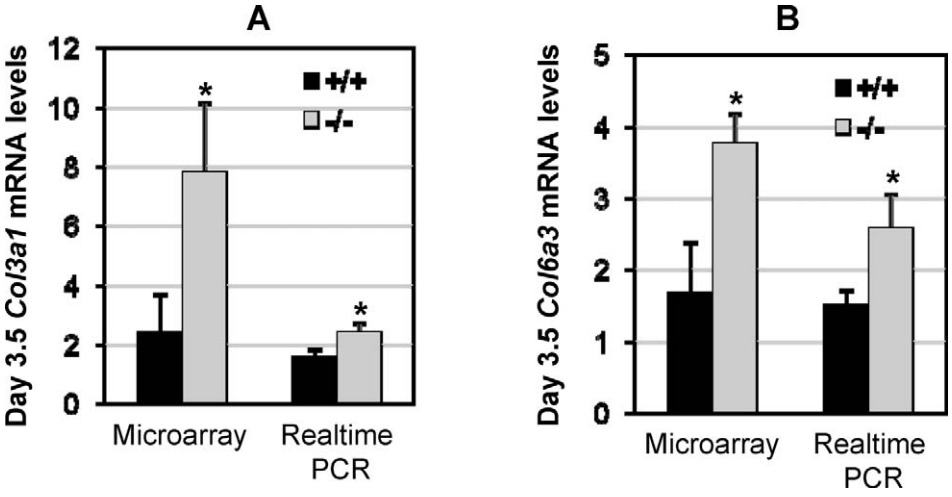

FIG. 2. Differential expression of *Col3a1* mRNA and *Col6a3* mRNA in Day 3.5 WT and *Lpar3*$^{-/-}$ uterus indicated by microarray and real-time PCR. **A**) *Col3a1* mRNA levels. **B**) *Col6a3* mRNA levels. Error bars represent standard deviation. *$P < 0.05$; n = 3 for microarray and n = 5–6 for real-time PCR; *Gapdh* was used as a loading control in the real-time PCR. Similar results were obtained when *Hprt1* was used as a loading control in the real-time PCR (data not shown).

TABLE 1. Summary of the effects of E2 and P4 on uterine COL III, I, VI, and IV expression.[a]

Collagen type	Effects	E2			P4		
		6 h	24 h	72 h	6 h	24 h	72 h
COL III	Thicker and longer fibrils	−	+	+	−	−	+
COL I	Thicker and longer fibrils	−	−	+	−	−	+/−
COL VI	Thicker and longer fibrils (+) and patchy fibrils (++)	+	+	++	+	+	+
COL IV	Reduced LE basement membrane	+	+	+	−	−	−

[a] −, not obvious; +, obvious.

web of immunoreactive COL VI became apparent and persisted after 24 hours of E2 or P4 treatment, and 72 h of P4 treatment (Supplemental Fig. S2, C, E, and F). However, after 72 h of E2 treatment, COL VI staining was patchy (Supplemental Fig. S2D), suggesting fibrillar aggregation. Supplemental Figure S3 demonstrates the regulation of COL IV by E2 and P4. COL IV was mainly detected in the walls of blood vessels and in epithelial basement membranes (Supplemental Fig. S3). Upon E2 treatment, COL IV stain in the LE basement membrane was reduced to barely detectable levels at all three time points examined (Fig. S3, C and D, and data not shown). However, P4 treatment did not affect COL IV expression in basement membrane, and neither E2 nor P4 affected the distribution of COL IV in blood vessels. Table 1 summarizes the effects of E2 and P4 on the expression of COL III, I, VI, and IV in the mouse uterus.

COL III Expression in Peri-Implantation WT and Lpar3$^{-/-}$ *Uterus*

Immunofluorescence demonstrates that, at Day 0.5, COL III was detected throughout the uterine endometrium and myometrium (Supplemental Fig. S4, C and D). COL III was not detected in LE or glandular epithelial (GE) cells, but reactivity was observed in the subepithelial ECM of both LE and GE (Supplemental Fig. S4, C and D). A similar distribution was observed at Day 3.5. There were no obvious differences between WT and *Lpar3*$^{-/-}$ in Day 0.5 and Day 3.5 uterus (Supplemental Figs. S4, C and D, and S5, A and B; Fig. 3, A and B).

Embryo implantation normally initiates around Day 4.0 in mice. In Day 4.5 uterus, COL III showed an expression pattern similar to Day 0.5 and Day 3.5 at low magnification (4×) (Supplemental Fig. S5, C and D), with the exception of a seemingly lighter stain in the primary decidual zone (Supplemental Fig. S5C). At higher magnification (20×), a reduced density of COL III with some discontinuities was seen in the stromal area in the Day 4.5 WT uterus (Fig. 3C) compared with that of Day 3.5 (Fig. 3A). Strong COL III staining was detected in the subepithelial ECM of LE in the WT uterus that was not adjacent to the primary decidual zone (Fig. 3C). The COL III stain in the subepithelial basement membrane area of LE in the Day 4.5 *Lpar3*$^{-/-}$ uterus was relatively even (Fig. 3D). The two embryos seen next to each other in the Day 4.5 *Lpar3*$^{-/-}$ uterus is an early indication of embryo crowding in the mutant (Fig. 3D) [30].

Subsequently, there was further disappearance of COL III from the decidual zone in Day 5.0 and Day 5.5 WT uterus, and significant clearance of COL III was also detected in the decidual zone of Day 5.5 *Lpar3*$^{-/-}$ uterus. In addition to more extensive COL III clearance in the Day 5.0 WT decidual zone compared with that in the Day 4.5 WT decidual zone (Fig. 3E and Supplemental Fig. S5E), higher magnification clearly showed almost parallel ''strings'' of COL III in the primary decidual zone surrounding the implanting embryo (Fig. 3E), oriented approximately parallel to an imaginary transverse line between mesometrium and antimesometrium (Fig. 3E and Supplemental Fig. S5E). In Day 5.5 WT uterus, the clearance of COL III was even more extensive, reaching almost the entire antimesometrial endometrium, with a low level of COL III staining still detectable in the junctional zone endometrium (Supplemental Fig. S5G). Meanwhile, the COL III strings present in the primary decidual zone at Day 5.0 were now detected in both mesometrial and antimesometrial sides of the implanting embryo, but not the decidual zone surrounding the embryo in the Day 5.5 uterus (Fig. 3G and Supplemental Fig. S5G). In Day 5.0 *Lpar3*$^{-/-}$ uterus, uneven and strong COL III stain in the subepithelial ECM of LE was detected (Fig. 3F and Supplemental Fig. S5F). In Day 5.5 *Lpar3*$^{-/-}$ uterus, disappearance of COL III from the primary decidual zone was evident (Supplemental Fig. S5H), although it was not as extensive as that in Day 5.0 and Day 5.5 WT uterus. Similar arrays of COL III strings to those seen in Day 5.0 WT implantation site were observed in the Day 5.5 *Lpar3*$^{-/-}$ uterus (Fig. 3H and Supplemental Fig. S5H). Intensive COL III stain remained in the myometrium in both the WT and *Lpar3*$^{-/-}$ uterus (Supplemental Fig. S5). COL III was not detected in embryos (Fig. 3, C–H).

COL VI Expression in Peri-Implantation WT and Lpar3$^{-/-}$ *Uterus*

In the preimplantation period (Days 0.5 and 3.5), intense COL VI staining was detected throughout the endometrium and myometrium (Supplemental Figs. S4, G and H, and S6, A and B), including the vasculature. No COL VI was detected in LE or GE, but reactivity was observed in the subepithelial ECM of both LE and GE (Fig. 4, A and B). No obvious difference in COL VI distribution was observed between WT and *Lpar3*$^{-/-}$ at Day 0.5 or 3.5 (Supplemental Figs. S4, G and H, and S6, A and B).

At Day 4.5, clearance of COL VI from the implantation site was observed in the WT uterus (Supplemental Fig. S6C), but this was not obvious in the *Lpar3*$^{-/-}$ uterus (Supplemental Fig. S6D). Higher magnification of Day 4.5 WT implantation sites indicated reduced COL VI staining in the primary decidual zone; immunoreactivity remained focally strong in blood vessel walls and adventitia, but lacked the circumferential continuity seen on earlier days. Uneven and discontinuous staining was also seen in the LE subepithelial ECM. No COL VI was detected in the embryo (Fig. 4, C–H). PECAM staining was used to visualize vascular endothelium and to confirm COL VI localization in and adjacent to vessel walls (Fig. 4J). These changes of COL VI distribution in decidual cells and ECM were not observed in the *Lpar3*$^{-/-}$ uterus where an embryo was present (Fig. 4D).

At Days 5.0 and 5.5, there was further COL VI clearance from extended areas in the WT implantation sites (Supplemental Fig. S6, E and G). Some slight evidence for clearance could now be observed in the subepithelial stroma next to the

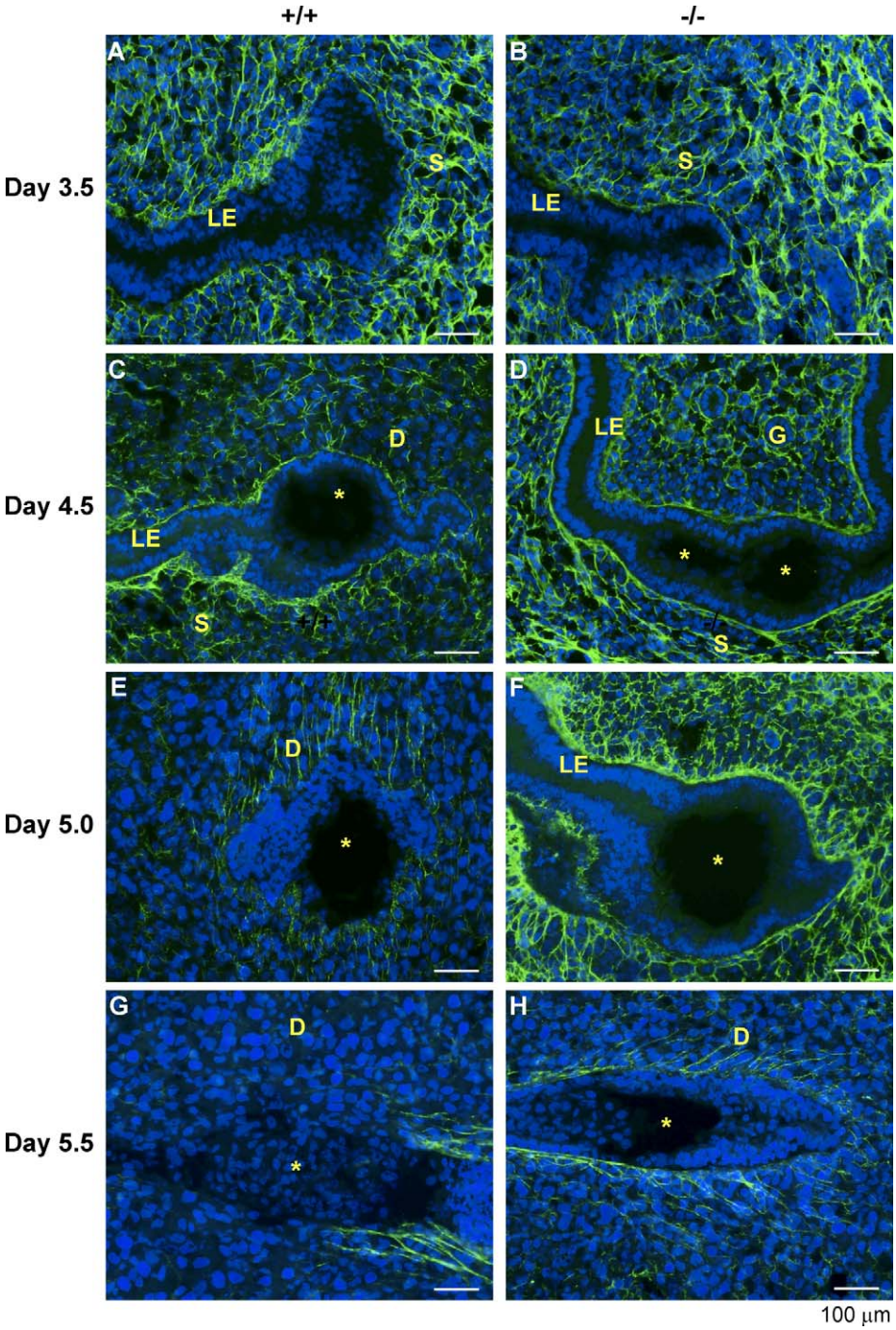

FIG. 3. COL III immunoreactivity in the WT and *Lpar3*$^{-/-}$ uterus from Day 3.5 to Day 5.5. Cross sections (10 μm) were cut on Day 3.5 and Day 5.5 uterus. Longitudinal sections (10 μm) were cut on Day 4.5 and Day 5.0 uterus in order to increase the chance of obtaining sections with embryos in the *Lpar3*$^{-/-}$ uterus. **A**) WT, Day 3.5. **B**) *Lpar3*$^{-/-}$, Day 3.5. **C**) WT, Day 4.5. **D**) *Lpar3*$^{-/-}$, Day 4.5. **E**) WT, Day 5.0. **F**) *Lpar3*$^{-/-}$, Day 5.0. **G**) WT, Day 5.5. **H**) *Lpar3*$^{-/-}$, Day 5.5. Green color represents COL III, blue represents DAPI to stain nucleus, and the yellow star indicates the embryo. D, decidual zone; G, glandular epithelium; S, stroma. Bar = 100 μm; n = 2–3.

embryo at Day 5.0 in *Lpar3*$^{-/-}$ uterus (Supplemental Fig. S6F), and further clearance was seen at Day 5.5 (Supplemental Fig. S6H). Higher magnification revealed disrupted COL VI staining in the subepithelial ECM and further COL VI breakdown in the decidualizing area in WT at Days 5.0 and 5.5 (Fig. 4, E and G). In the junctional zone endometrium of Day 5.5 WT uterus, COL VI was still present around the stromal cells and beneath GE basement membranes (Fig. 4I and Supplemental Fig. S6G). Similar changes of COL VI distribution associated with the progress of implantation were observed in Day 5.0 and Day 5.5 *Lpar3*$^{-/-}$ sites, except that these changes were delayed compared with the same day in WT (Fig. 4, E–H). Although COL VI reactivity disappeared from the decidualizing cells, some staining remained in the walls of blood vessels in implantation sites (Fig. 4, C–F, and Supplemental Fig. S6, C–H).

COL I Expression in Peri-Implantation WT and Lpar3$^{-/-}$ *Uterus*

Like COL III, COL I is a type of fibril-forming collagen, but microarray analysis did not show differential expression of *Col I* in the Day 3.5 *Lpar3*$^{-/-}$ uterus (data not shown). For comparison, we examined COL I expression in the peri-implantation WT and *Lpar3*$^{-/-}$ uterus. The distribution of COL I (Fig. 5, A and B, and Supplemental Figs. S4, A and B, and S7, A and B) was very similar to COL III (Fig. 3, A and B, and Supplemental Figs. S4, C and D, and S5A) at Days 0.5 and 3.5,

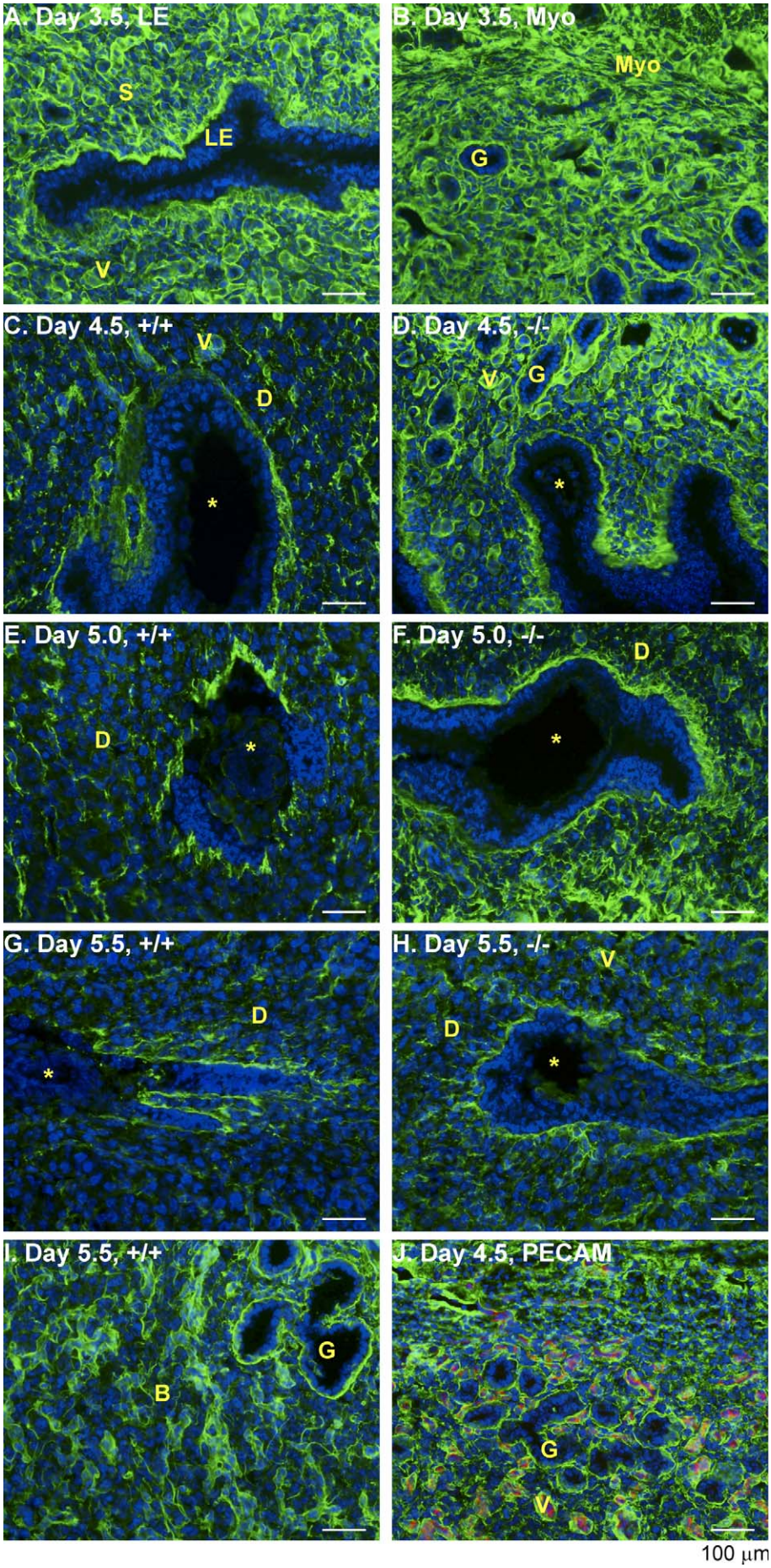

FIG. 4. Spatiotemporal expression of COL VI in the WT and *Lpar3*$^{-/-}$ uterus. Fresh frozen uterine cross sections (Day 3.5 and Day 5.5) and longitudinal sections (Day 4.5 and Day 5.0) were cut at 10 μm. **A**) Day 3.5 uterus to highlight LE and stroma. **B**) Day 3.5 uterus to highlight GE and myometrium; there is no obvious difference in the COL VI labeling between Day 3.5 WT and *Lpar3*$^{-/-}$ uterus. **C**) WT, Day 4.5. **D**) *Lpar3*$^{-/-}$, Day 4.5. **E**) WT, Day 5.0. **F**) *Lpar3*$^{-/-}$, Day 5.0. **G**) WT, Day 5.5. **H**) *Lpar3*$^{-/-}$, Day 5.5. Green color represents COL VI, blue represents DAPI, red represents PECAM, and the yellow star indicates the embryo. B, basal endometrium; D, decidual zone; G, glandular epithelium; Myo, myometrium; S, stroma; V, vasculature. Bar = 100 μm; n = 2–3.

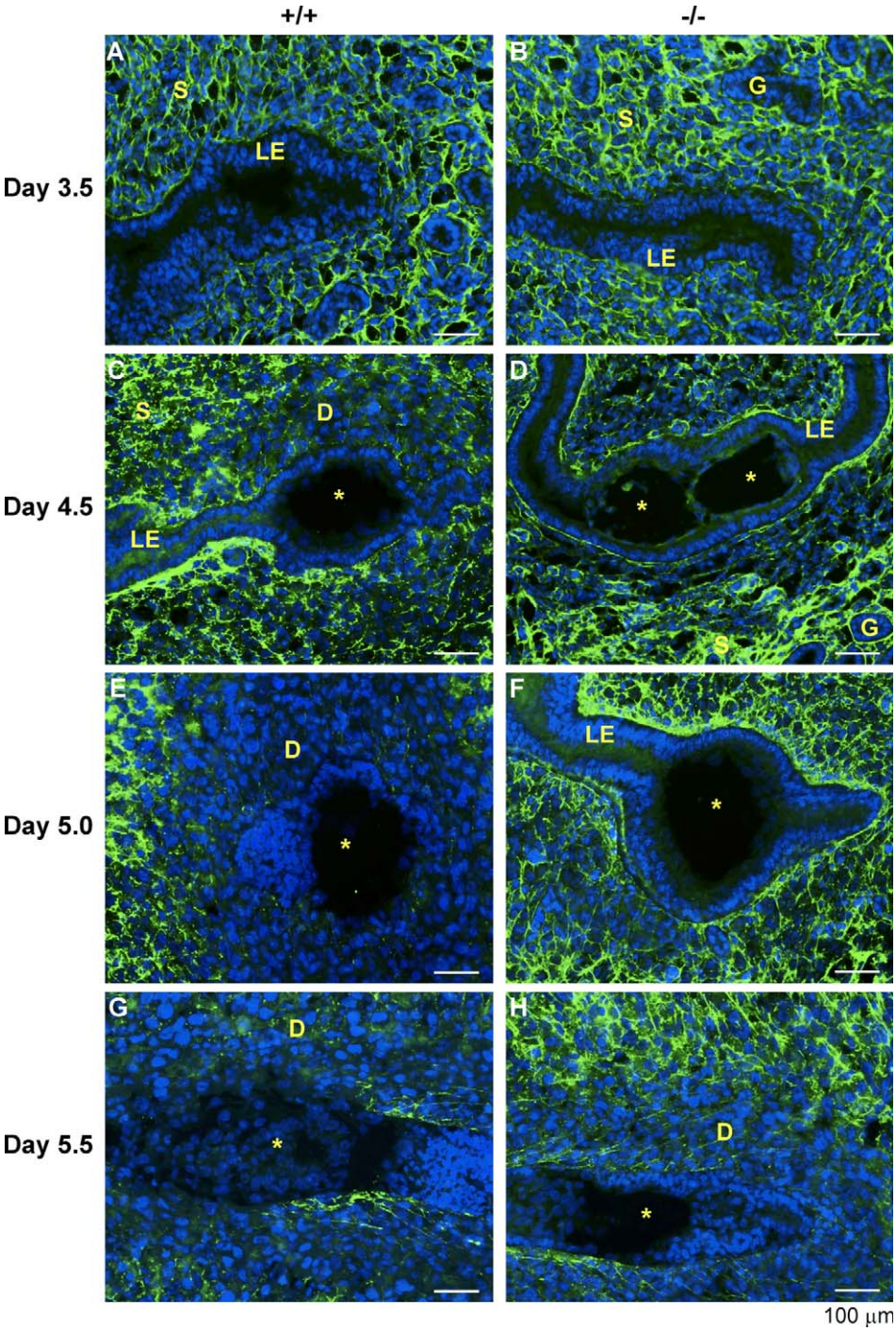

FIG. 5. Distribution of COL I immunoreactivity in the WT and *Lpar3*$^{-/-}$ uterus from Day 3.5 to Day 5.5. Fresh-frozen uterine cross sections (Days 3.5 and 5.5) and longitudinal sections (Days 4.5 and 5.0) were cut at 10 μm. **A**) WT, Day 3.5. **B**) *Lpar3*$^{-/-}$, Day 3.5. **C**) WT, Day 4.5. **D**) *Lpar3*$^{-/-}$, Day 4.5. **E**) WT, Day 5.0. **F**) *Lpar3*$^{-/-}$, Day 5.0. **G**) WT, Day 5.5. **H**) *Lpar3*$^{-/-}$, Day 5.5. Blue color indicates DAPI, green represents COL I, and the yellow star indicates the embryo. D, decidual zone; G, glandular epithelium; LE, luminal epithelium; S, stroma. Bar = 100 μm; n = 2–3.

and there was no obvious difference between WT and *Lpar3*$^{-/-}$ uterus at either time point. As with COL III, intensive COL I stain remained in the myometrium in both WT and *Lpar3*$^{-/-}$ uterus (Supplemental Fig. S7), and COL I was not detected in the embryos (Fig. 5, C–H).

However, compared with COL III, the clearance of COL I from the implantation site was delayed and not as extensive (Fig. 5, C–H, and Supplemental Fig. S7) from Day 4.5 to Day 5.5, either in WT or *Lpar3*$^{-/-}$ uterus. There was discontinuous COL I staining in Day 5.5 WT decidual zone (Fig. 5G), whereas COL III had already disappeared in Day 5.5 WT decidual zone (Fig. 3G). In addition, there were COL III strings detected in the primary decidual zone at Day 5.0 (Fig. 3E), but no obvious COL I-positive strings were observed in Day 5.0 WT implantation site (Fig. 5E), suggesting that COL I is not part of these string structures.

COL IV Expression in the Peri-Implantation WT and Lpar3$^{-/-}$ *Uterus*

For purposes of comparison, we also examined the major basement membrane collagen, COL IV, the mRNA level for which was not different between Day 3.5 WT and *Lpar3*$^{-/-}$ uterus in the microarray analysis (data not shown).

In the Preimplantation Days 0.5 and 3.5 uterus, COL IV was highly expressed in the myometrium, vasculature, and the LE and GE basement membranes, with most intensive labeling in the vasculature; low levels were also detectable in interstitial

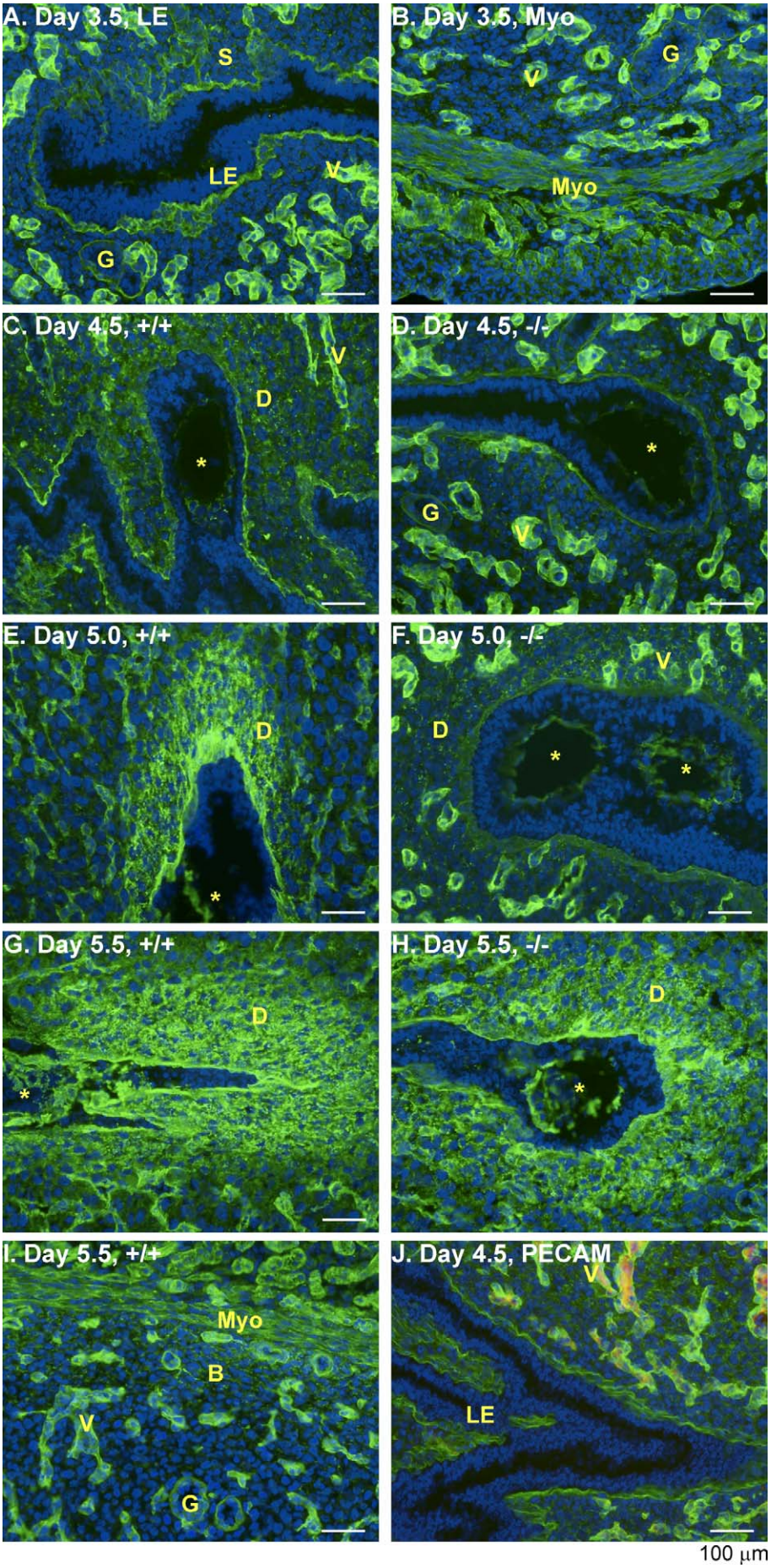

FIG. 6. Immunolabeling of COL IV in the WT and *Lpar3*$^{-/-}$ uterus. Fresh-frozen uterine cross sections (Days 3.5 and 5.5) and longitudinal sections (Days 4.5 and 5.0) were cut at 10 μm. **A**) Day 3.5 uterus to highlight LE, GE, and stroma. **B**) Day 3.5 uterus to highlight myometrium, blood vessel, and GE; there is no obvious difference in the COL IV labeling between Day 3.5 WT and *Lpar3*$^{-/-}$ uterus. **C**) WT, Day 4.5. **D**) *Lpar3*$^{-/-}$, Day 4.5. **E**) WT, Day 5.0. **F**) *Lpar3*$^{-/-}$, Day 5.0. **G**) WT, Day 5.5. **H**) *Lpar3*$^{-/-}$, Day 5.5. Green color represents COL IV, blue represents DAPI, red represents PECAM, and the yellow star indicates the embryo. B, basal endometrium; D, decidual zone; G, glandular epithelium; Myo, myometrium; S, stroma; V, vasculature. Bar = 100 μm; n = 2–3.

areas of the endometrium. Staining was absent from LE and GE cells. No obvious differences in COL IV expression patterns were observed between WT and *Lpar3*$^{-/-}$ at Days 0.5 or 3.5 (Fig. 6, A and B, and Supplemental Figs. S4, E and F, and S8, A and B).

In the Day 4.5 WT uterus, reduced COL IV staining was observed in the LE basement membrane next to the primary decidual zone, which, in contrast, seemed to have increased COL IV stain; faint staining was also observed in the embryo (Fig. 6C). Although the distribution of blood vessels in the endometrium changed upon implantation, the intensity of COL IV reactivity in the vasculature and myometrium did not seem to change (Fig. 6C and Supplemental Fig. S8C). These changes were not observed in the Day 4.5 *Lpar3*$^{-/-}$ uterus where an embryo was present; in keeping with the intact epithelial layer seen in histology (Fig. 1B), continuous LE basement membrane staining persisted (Fig. 6D and Supplemental Fig. S8D). Faint COL IV staining was observed in Day 4.5 embryos (Fig. 6, C and D).

In the Day 5.0 and 5.5 WT uterus, two prominent changes were observed: one was the appearance of intensive COL IV staining in the primary decidual zone extending several cells layers below the embryo; the other was increased staining in the embryo itself (Fig. 6, E and G, and Supplemental Fig. S8, E and G). Higher-magnification examination revealed granular staining, both intracellular and extracellular (Fig. 6, E and G). At Day 5.5, the embryo was intensively stained (Fig. 6G and Supplemental Fig. S8G). These changes of COL IV staining were not obvious in *Lpar3*$^{-/-}$ uterus at Day 5.0 (Fig. 6F and Supplemental Fig. S8F), but manifested at Day 5.5 (Fig. 6H and Supplemental Fig. S8H), which is consistent with the effect of delayed embryo implantation. Figure 6I shows COL IV staining in the basal endometrium and myometrium in Day 5.5 WT uterus, with immunoreactivity mainly in the vasculature, myometrium, and GE basement membrane. Figure 6J confirms that COL IV and PECAM were coexpressed in the blood vessels, but not other areas.

Differential Expression of Serine Proteases and MMPs in Day 3.5 Lpar3$^{-/-}$ *Uterus*

Collagen turnover is regulated by various factors, including serine proteases and MMPs [1, 35–37]. In line with the differential expression of *Col3a1* and *Col6a3* in the Day 3.5 *Lpar3*$^{-/-}$ uterus, microarray analysis indicated downregulation of several genes encoding serine proteases and MMPs that have roles in collagen degradation and ECM turnover. Differential expression of *Cma1* (mast cell chymase 1/mast cell protease 1/mast cell protease 5/Mcp5/Mcpt5), *Mcp4* (mast cell protease 4/Mcpt4), *Mcp6* (mast cell protease 6/Mcpt6), *Mmp3*, and *Mmp7* on Day 3.5 was confirmed using real-time PCR (Fig. 7).

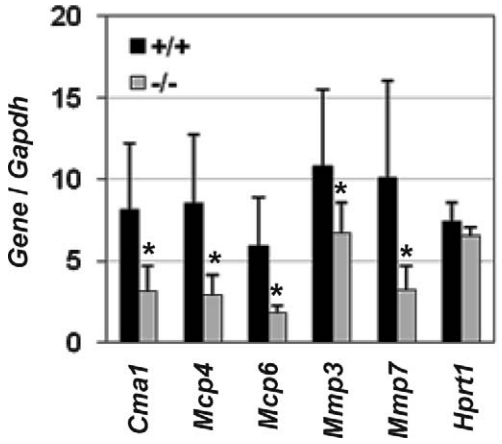

FIG. 7. Real-time PCR confirming several genes involved in collagen turnover indicated by microarray in Day 3.5 WT (+/+) and *Lpar3*$^{-/-}$ uterus. *Hprt1* is a house keeping gene used as an additional control. Error bars represent standard deviation. *$P < 0.05$; n = 5–6; *Gapdh* was used as a loading control. *Cma1*, mast cell chymase 1/mast cell protease 1/mast cell protease 5/Mcp5/Mcpt5; *Mcp4*, mast cell protease 4/Mcpt4; *Mcp6*, mast cell protease 6/Mcpt6.

DISCUSSION

The regulation of COL I, III, IV, and VI by E2 and P4, as well as the spatiotemporal expression patterns of these four collagen types, were systemically examined in the ovariectomized and the peri-implantation mouse uterus. Each of these collagen types has a distinct spatiotemporal regulation pattern by E2 and P4, and a unique, dynamic pattern of expression in the uterus in early pregnancy. All four collagen types are expressed in the stroma and myometrium, but are undetectable in the LE and GE during peri-implantation. COL I, III, and VI have a discontinuous appearance in the oil-treated ovariectomized uterus. Both E2 and P4 treatments produce thicker and longer fibrils and a web-like appearance, although, overall, the effects of E2 precede those of P4 (Table 1 and Supplemental Figs. S1 and S2). One study indicates that the abundance of COL I correlates with the serum E2 level, but not the P4 level, in the naturally cycling mouse uterus [38]. The effects of E2 and P4 on COL IV are distinctly different from those on COL I, III, and VI. E2 treatment does not affect the expression of COL IV in the vasculature, but reduces its expression in basement membranes, while P4 does not have an obvious effect on COL IV expression (Supplemental Fig. S3). These results are inconsistent with the data from natural estrous cycle, in which the degradation of COL IV from LE basement membrane is correlated with serum P4, but not E2 levels [38]. In preimplantation uterus, COL I, III, and VI take on a web-like distribution (Figs. 3–5), most likely reflecting the combined effects of E2 and P4 on ECM (Supplemental Figs. S1 and S2). In addition, COL IV staining in the LE basement membrane is much weaker than in the vasculature (Fig. 6A and Supplemental Fig. S4E), whereas, in oil-treated ovariectomized uterus, the COL IV staining in the LE basement membrane is equally intense as that in the vasculature (Supplemental Fig. S3, A and B), perhaps reflecting the effect of E2 on COL IV expression in the LE basement membrane (Supplemental Fig. S3, C and D). During peri-implantation, COL I, III, and VI disappear from the decidual zone upon embryo implantation, and are undetectable in the embryo (Figs. 3–5) [34]. In contrast, COL IV accumulates in the decidual zone, and is highly expressed in embryonic basement membranes (Fig. 6).

COL I and COL III are fibril-forming collagens. They have the closest expression patterns among the four examined collagen types in the WT peri-implantation uterus, and they both have been reported to disappear from the implantation site [5, 6]. However, the clearance of COL I from the implantation site is not as fast and extensive as that of COL III (Figs. 3 and 5, and Supplemental Figs. S5 and S7). These results agree with those of another study in rat uterus that shows 30% and 55% clearance of COL I and COL III, respectively, in the implantation site from Day 5.5 to Day 6.5; and 16% and 31% clearance of COL I and COL III, respectively, in the implantation site from Day 6.5 to Day 7.5 [6]. Previous studies in the mouse indicate weaker COL III staining on Day 5 than on later days [7], with reorganization into sparsely distributed, thick intercellular fibrils by Day 7 [39].

The expression pattern of COL IV differs from that of the other three collagen types. It has been previously reported that COL IV disappears from the LE basement membrane and appears in the embryo during implantation [9], which is consistent with our results (Fig. 6 and Supplemental Fig. S8). The accumulation of COL IV protein in the decidual zone (Fig. 6 and Supplemental Fig. S8) is also consistent with the reported *Col4a1* mRNA and COL IV protein expression in the same area [9, 10]. COL IV consistently has intensive expression in the blood vessels in the peri-implantation mouse uterus (Fig. 6 and Supplemental Fig. S8). COL VI is also detected in the blood vessels, but its relative expression level is not as intensive as that of COL IV when compared with the expression levels in other uterine compartments. Interestingly, COL VI degradation in decidua is spatially restricted, not extending to the vessel walls (Fig. 4 and Supplemental Fig. S6). A similar phenomenon occurs in both rat and human decidua [11, 40]. This probably reflects the role of COL VI, which seems to envelop vessels, perhaps as a way of integrating them into the surrounding three-dimensional tissue architecture.

These spatiotemporal changes in COL I, III, IV, and VI in the *Lpar3*$^{-/-}$ peri-implantation mouse uterus are all delayed compared with that in the WT peri-implantation uterus (Figs. 3–6, and Supplemental Figs. S5–S8). These changes were different from the effects of E2 and P4 on uterine collagen expression in ovariectomized WT uterus, indicating that the altered collagen expression in *Lpar3*$^{-/-}$ uterus is unlikely to be a result of alterations in ovarian hormones. The statement is supported by our observation that there is no significant difference in serum E2 and P4 levels between WT and *Lpar3*$^{-/-}$ mice on Day 3.5 and Day 4.5 (data not shown). One explanation for retention of COL III and COL VI in the *Lpar3*$^{-/-}$ implantation sites could be higher mRNA expression levels (Fig. 2), leading to elevated rates of protein synthesis and, possibly, more abundant ECM collagen, although this was not apparent in the immunostaining at Day 3.5. In addition, decreased uterine expression of genes involved in ECM turnover, including mast cell proteases and MMPs (Fig. 7), may very well contribute importantly to the delayed clearance of COL I, III, and VI in *Lpar3*$^{-/-}$ uterus [20, 37]. COL VI is resistant to some of the major MMPs; however, it can be degraded by mast cell chymases and some other serine proteinase matrix-degrading enzymes [21]. Mast cell chymase can also regulate the activities of pro-MMP-2 and -9; as well as inhibit the expression of *Col I* and *Col III* mRNA [23, 41]. It seems that COL IV is synthesized in the decidual cells [9, 10], so the delayed accumulation of COL IV may reflect delayed implantation in *Lpar3*$^{-/-}$ uterus (Fig. 6 and Supplemental Fig. S8), with delayed onset of de novo gene expression and production of COL IV in the decidual zone.

How is LPA3 involved in regulating collagen metabolism? *Lpar3* is mainly expressed in the LE [30], where none of the collagen types that we have examined are detected (Fig. 3–6) [34]. Thus, LE may not be a main source for collagen synthesis in the period under study. The LE-specific localization of *Lpar3* suggests that LPA3 may have a paracrine effect on collagen regulation [42]. Since LE is the first layer of cells with which an implanting embryo communicates, if LPA3 mediates the communication between an implanting embryo and the stromal cells, its absence could lead to a delay in the molecular program of primary decidual differentiation.

Dysregulation of uterine ECM turnover has been associated with uterine dysfunction, including defective uterine receptivity. Overproduction of human mast cell chymase in the myometrium may be involved in the pathogenesis of severe pre-eclampsia [43]. Reduced COL IV expression in human decidual tissues may be associated with spontaneous abortion [44]. Reduced COL IV expression in the endometrium of women postluteinizing hormone surge was associated with unexplained infertility [45]. Decreased levels of MMP9 and tissue inhibitor of MMP (TIMP) 1 were detected in uterine fluid during the expected implantation window in women with infertility and unexplained recurrent miscarriage [46]. Decreased uterine receptivity is a main reason for the low pregnancy rate and higher miscarriage rate in patients with polycystic ovary syndrome (PCOS). It has been demonstrated that *Mmp26* is downregulated in the uterus of PCOS patients during the expected implantation window [47]. Compared to normal midsecretory endometrium (expected implantation window), higher mRNA levels of *Col I*, *Mmp2*, and cathepsin H, as well as lower mRNA levels of *Timp3* were detected in midsecretory endometrium of patients with unexplained infertility and/or recurrent miscarriages [48].

This study demonstrates that deletion of *Lpar3* leads to altered spatiotemporal expression of COL I, III, IV, and VI in the peri-implantation uterus. These changes are in line with the delayed uterine receptivity in the *Lpar3*$^{-/-}$ uterus. However, the functional significance of these collagen types in the *Lpar3*$^{-/-}$ mice is currently unknown. We speculate that altered collagen expression could contribute to delayed implantation and subfertility in *Lpar3*$^{-/-}$ mice.

ACKNOWLEDGMENTS

The authors thank Dr. James N. Moore and Dr. Zhen Fu at the College of Veterinary Medicine, University of Georgia for the access to the ABI 7900 Real-Time PCR machine and the imaging system, respectively, the University of Georgia Center for Advanced Ultrastructural Research for access to the fluorescent microscope, and the Genomics and Proteomics Core Facility Medical College of Georgia for the microarray analysis.

REFERENCES

1. Aplin JD. Endometrial extracellular matrix. In: Aplin JD, Fazleabas AT, Glasser SR, and Giudice LC (eds.), The Endometrium: Molecular, Cellular, and Clinical Perspectives, 2nd ed. London, United Kingdom: Informa Healthcare; 2008:364–378.
2. Heino J. The collagen family members as cell adhesion proteins. Bioessays 2007; 29:1001–1010.
3. Morrione TG, Seifter S. Alteration in the collagen content of the human uterus during pregnancy and post partum involution. J Exp Med 1962; 115:357–365.
4. Hurst PR, Gibbs RD, Clark DE, Myers DB. Temporal changes to uterine collagen types I, III and V in relation to early pregnancy in the rat. Reprod Fertil Dev 1994; 6:669–677.
5. Clark DE, Hurst PR, McLennan IS, Myers DB. Immunolocalization of collagen type I and laminin in the uterus on Days 5 to 8 of embryo implantation in the rat. Anat Rec 1993; 237:8–20.
6. Hurst PR, Palmay RD, Myers DB. Localization and synthesis of collagen types III and V during remodelling and decidualization in rat uterus. Reprod Fertil Dev 1997; 9:403–409.
7. Spiess K, Teodoro WR, Zorn TM. Distribution of collagen types I, III, and V in pregnant mouse endometrium. Connect Tissue Res 2007; 48:99–108.
8. Armant DR, Kameda S. Mouse trophoblast cell invasion of extracellular matrix purified from endometrial tissue: a model for peri-implantation development. J Exp Zool 1994; 269:146–156.
9. Blankenship TN, Given RL. Loss of laminin and type IV collagen in uterine luminal epithelial basement membranes during blastocyst implantation in the mouse. Anat Rec 1995; 243:27–36.
10. Farrar JD, Carson DD. Differential temporal and spatial expression of mRNA encoding extracellular matrix components in decidua during the peri-implantation period. Biol Reprod 1992; 46:1095–1108.
11. Mulholland J, Aplin JD, Ayad S, Hong L, Glasser SR. Loss of collagen type VI from rat endometrial stroma during decidualization. Biol Reprod 1992; 46:1136–1143.

12. Rahima A, Soderwall AL. Uterine collagen content in young and senescent pregnant golden hamsters. J Reprod Fertil 1977; 49:161–162.
13. Ryan JN, Woessner JF Jr. Oestradiol inhibits collagen breakdown in the involuting rat uterus. Biochem J 1972; 127:705–713.
14. Ryan JN, Woessner JF Jr. Oestradiol inhibition of collagenase role in uterine involution. Nature 1974; 248:526–528.
15. Koob TJ, Jeffrey JJ. Hormonal regulation of collagen degradation in the uterus: inhibition of collagenase expression by progesterone and cyclic AMP. Biochim Biophys Acta 1974; 354:61–70.
16. Pan Y, Liu Z, Zhu C. Effect of mifepristone on the expression of chorionic gonadotropin beta subunit and collagen type IV in female rhesus monkey decidua and villus at early gestation [in Chinese]. Zhonghua Nan Ke Xue 2004; 10:358–361, 365.
17. Rodriguez HA, Kass L, Varayoud J, Ramos JG, Ortega HH, Durando M, Munoz-De-Toro M, Luque EH. Collagen remodelling in the guinea-pig uterine cervix at term is associated with a decrease in progesterone receptor expression. Mol Hum Reprod 2003; 9:807–813.
18. Rodriguez HA, Ramos JG, Ortega HH, Munoz-de-Toro M, Luque EH. Regional changes in the spatio-temporal pattern of progesterone receptor (PR) expression in the guinea-pig genital tract as parturition approaches. J Steroid Biochem Mol Biol 2008; 111:247–254.
19. Alexander CM, Hansell EJ, Behrendtsen O, Flannery ML, Kishnani NS, Hawkes SP, Werb Z. Expression and function of matrix metalloproteinases and their inhibitors at the maternal-embryonic boundary during mouse embryo implantation. Development 1996; 122:1723–1736.
20. Curry TE Jr, Osteen KG. The matrix metalloproteinase system: changes, regulation, and impact throughout the ovarian and uterine reproductive cycle. Endocr Rev 2003; 24:428–465.
21. Kielty CM, Lees M, Shuttleworth CA, Woolley D. Catabolism of intact type VI collagen microfibrils: susceptibility to degradation by serine proteinases. Biochem Biophys Res Commun 1993; 191:1230–1236.
22. Kofford MW, Schwartz LB, Schechter NM, Yager DR, Diegelmann RF, Graham MF. Cleavage of type I procollagen by human mast cell chymase initiates collagen fibril formation and generates a unique carboxyl-terminal propeptide. J Biol Chem 1997; 272:7127–7131.
23. Tchougounova E, Lundequist A, Fajardo I, Winberg JO, Abrink M, Pejler G. A key role for mast cell chymase in the activation of pro-matrix metalloprotease-9 and pro-matrix metalloprotease-2. J Biol Chem 2005; 280:9291–9296.
24. Abe M, Ho CH, Kamm KE, Grinnell F. Different molecular motors mediate platelet-derived growth factor and lysophosphatidic acid-stimulated floating collagen matrix contraction. J Biol Chem 2003; 278:47707–47712.
25. Watterson KR, Lanning DA, Diegelmann RF, Spiegel S. Regulation of fibroblast functions by lysophospholipid mediators: potential roles in wound healing. Wound Repair Regen 2007; 15:607–616.
26. Sato M, Shegogue D, Hatamochi A, Yamazaki S, Trojanowska M. Lysophosphatidic acid inhibits TGF-beta-mediated stimulation of type I collagen mRNA stability via an ERK-dependent pathway in dermal fibroblasts. Matrix Biol 2004; 23:353–361.
27. Fishman DA, Liu Y, Ellerbroek SM, Stack MS. Lysophosphatidic acid promotes matrix metalloproteinase (MMP) activation and MMP-dependent invasion in ovarian cancer cells. Cancer Res 2001; 61:3194–3199.
28. Mutoh T, Chun J. Lysophospholipid activation of G protein-coupled receptors. Subcell Biochem 2008; 49:269–297.
29. Choi JW, Herr DR, Noguchi K, Yung YC, Lee CW, Mutoh T, Lin ME, Teo ST, Park KE, Mosley AN, Chun J. LPA receptors: subtypes and biological actions. Annu Rev Pharmacol Toxicol 2010; 50:157–186.
30. Ye X, Hama K, Contos JJ, Anliker B, Inoue A, Skinner MK, Suzuki H, Amano T, Kennedy G, Arai H, Aoki J, Chun J. LPA3-mediated lysophosphatidic acid signalling in embryo implantation and spacing. Nature 2005; 435:104–108.
31. Hama K, Aoki J, Inoue A, Endo T, Amano T, Motoki R, Kanai M, Ye X, Chun J, Matsuki N, Suzuki H, Shibasaki M, Arai H. Embryo spacing and implantation timing are differentially regulated by LPA3-mediated lysophosphatidic acid signaling in mice. Biol Reprod 2007; 77:954–959.
32. Pelch KE, Schroder AL, Kimball PA, Sharpe-Timms KL, Davis JW, Nagel SC. Aberrant gene expression profile in a mouse model of endometriosis mirrors that observed in women. Fertil Steril 2010; 93: 1615–1627.
33. Ye X, Skinner MK, Kennedy G, Chun J. Age-dependent loss of sperm production in mice via impaired lysophosphatidic acid signaling. Biol Reprod 2008; 79:328–336.
34. Dziadek M, Darling P, Zhang RZ, Pan TC, Tillet E, Timpl R, Chu ML. Expression of collagen alpha 1(VI), alpha 2(VI), and alpha 3(VI) chains in the pregnant mouse uterus. Biol Reprod 1995; 52:885–894.
35. Song F, Wisithphrom K, Zhou J, Windsor LJ. Matrix metalloproteinase dependent and independent collagen degradation. Front Biosci 2006; 11: 3100–3120.
36. Trackman PC. Diverse biological functions of extracellular collagen processing enzymes. J Cell Biochem 2005; 96:927–937.
37. Lauer-Fields JL, Juska D, Fields GB. Matrix metalloproteinases and collagen catabolism. Biopolymers 2002; 66:19–32.
38. Wood GA, Fata JE, Watson KL, Khokha R. Circulating hormones and estrous stage predict cellular and stromal remodeling in murine uterus. Reproduction 2007; 133:1035–1044.
39. Spiess K, Zorn TM. Collagen types I, III, and V constitute the thick collagen fibrils of the mouse decidua. Microsc Res Tech 2007; 70:18–25.
40. Aplin JD, Charlton AK, Ayad S. An immunohistochemical study of human endometrial extracellular matrix during the menstrual cycle and first trimester of pregnancy. Cell Tissue Res 1988; 253:231–240.
41. Wang Y, Shiota N, Leskinen MJ, Lindstedt KA, Kovanen PT. Mast cell chymase inhibits smooth muscle cell growth and collagen expression in vitro: transforming growth factor-beta1-dependent and -independent effects. Arterioscler Thromb Vasc Biol 2001; 21:1928–1933.
42. Xie Y, Gibbs TC, Meier KE. Lysophosphatidic acid as an autocrine and paracrine mediator. Biochim Biophys Acta 2002; 1582:270–281.
43. Mitani R, Maeda K, Fukui R, Endo S, Saijo Y, Shinohara K, Kamada M, Irahara M, Yamano S, Nakaya Y, Aono T. Production of human mast cell chymase in human myometrium and placenta in cases of normal pregnancy and preeclampsia. Eur J Obstet Gynecol Reprod Biol 2002; 101:155–160.
44. Iwahashi M, Muragaki Y, Ooshima A, Nakano R. Decreased type IV collagen expression by human decidual tissues in spontaneous abortion. J Clin Endocrinol Metab 1996; 81:2925–2929.
45. Bilalis DA, Klentzeris LD, Fleming S. Immunohistochemical localization of extracellular matrix proteins in luteal phase endometrium of fertile and infertile patients. Hum Reprod 1996; 11:2713–2718.
46. Skrzypczak J, Wirstlein P, Mikolajczyk M. Could the defects in the endometrial extracellular matrix during the implantation be a cause for impaired fertility? Am J Reprod Immunol 2007; 57:40–48.
47. Qiao J, Wang L, Li R, Zhang X. Microarray evaluation of endometrial receptivity in Chinese women with polycystic ovary syndrome. Reprod Biomed Online 2008; 17:425–435.
48. Jokimaa V, Oksjoki S, Kujari H, Vuorio E, Anttila L. Altered expression of genes involved in the production and degradation of endometrial extracellular matrix in patients with unexplained infertility and recurrent miscarriages. Mol Hum Reprod 2002; 8:1111–1116.